International Research Journal of Advanced Engineering and Science
ISSN (Online): 2455-9024

Photovoltaic Power Injected into Low Voltage Grid Using P/Q Regulation Method

Andry Thierry RANDRIANARINOSY[1], Jean Marc Fabien Sitraka RANDRIANIRINA, Eulalie RAFANJANIRINA, Zely Arivelo RANDRIAMANATANY
Faculty of Sciences, University of Antananarivo

Abstract: *In the context of energy transition, integrating photovoltaic generation into Madagascar's low voltage (LV) grid represents a sustainable alternative to the country's insufficient energy supply. However, unregulated power injection causes significant disturbances such as voltage fluctuations, reactive power injection, and harmonic currents, which compromise grid stability. This study proposes a control strategy based on P/Q regulation, modeled in Matlab/Simulink, to manage the active and reactive power injected into the grid. Numerical simulations validated the relevance of this approach: the active power injected reaches 99.97% of the PV field production, voltage THD is reduced to 4.29%, frequency is stabilized at* $50\,Hz \pm 0.1\,Hz$*, and the power factor is improved up to 0.99. These results confirm the effectiveness of the method for integration in compliance with the Malagasy GRID-CODE standards.*

Keywords: *Low Voltage Grid, P/Q Control, Photovoltaic, Power Injection, Power Quality*

I. Introduction

Global electricity demand is continuously increasing, [1]. At the same time, fossil resources are becoming scarce and causing environmental issues, [2]. This situation is pushing countries to rapidly adopt renewable energy sources.

In Madagascar, this reality is reflected in frequent power outages. The electrical grid cannot meet the population's needs. Yet, the country benefits from high solar irradiation, with solar potential exceeding 2000 kWh/m²/year, [3]. This makes solar energy a sustainable and locally appropriate solution.

However, integrating this energy into the low voltage grid presents challenges, [4]. If power injection is not properly controlled, it can deteriorate power quality. It causes voltage fluctuations, generates harmonic currents, and introduces unwanted reactive power. All of these effects compromise grid stability.

Similar P/Q control strategies have been successfully deployed in Brazilian, Indian, and sub-Saharan African rural grids where voltage stability and reactive power mitigation are essential for PV integration [5].

This study aims to better manage solar energy injection using a P/Q regulation method to control active and reactive power. This regulation complies with the quality standards defined in the Malagasy GRID-CODE.

The system under study includes several components: a photovoltaic field, a Boost converter with a Perturbation & Observation (P&O) MPPT algorithm, a three-phase inverter, an LCL filter, and a P/Q regulator. All components are simulated in the Matlab/Simulink environment.

The objective is to determine whether this regulation ensures stable and compliant power injection without degrading the quality of electricity delivered to the grid.

II. Modeling of PV System Components

A. Photoelectric Effect

Solar energy captured by PV modules originates from the sun's radiation, which results from nuclear fusion reactions occurring in its core, [6]. This radiation consists of photons whose energy is given by the relation:

$$Eph = h\frac{C}{\lambda} \qquad (1)$$

where h is Planck's constant, c is the speed of light, and λ is the wavelength.

The photovoltaic conversion principle is based on the photoelectric effect observed in PN junctions (one side doped P-type with boron atoms in the silicon lattice, the other side doped N-type with phosphorus atoms). The absorption of photons by the semiconductors generates electron-hole pairs, which are then collected to produce an electric current.

B. PV Cell Model

The electrical model of a PV cell is represented by a single-diode model: a current source, a diode, a series resistance R_s, and a shunt resistance R_{sh}, [7].

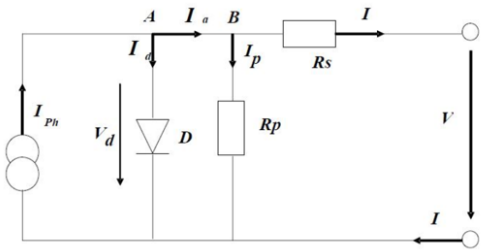

Figure 1: The electrical model of a PV

In this equivalent circuit, the PV cell is considered as a current source due to the photoelectric effect. The output current is given by:

$$I = I_{ph} - I_0\left(e^{\frac{q(V+IR_s)}{nkT}} - 1\right) - \frac{V+IR_s}{R_{sh}} \qquad (2)$$

Where I is the output current of the cell, I_{ph} is the current generated by the photoelectric effect, I_0 is the diode saturation current, R_s is the series resistance, V is the terminal voltage, T is the temperature, and n is the diode ideality factor.

The power $P(V)$ and current $I(V)$ delivered by a photovoltaic cell can be expressed as functions of the terminal

Andry Thierry RANDRIANARINOSY, Jean Marc Fabien Sitraka RANDRIANIRINA, Falinirina ANDRIANJATOVO, and Zely Arivelo RANDRIAMANATANY, "Photovoltaic Power Injected into Low Voltage Grid Using P/Q Regulation Method," *International Research Journal of Advanced Engineering and Science*, Volume 10, Issue 4, pp. 9-15, 2025.

International Research Journal of Advanced Engineering and Science
ISSN (Online): 2455-9024

voltage. By implementing the equations (2) in the Matlab/Simulink software and maintaining a constant temperature, the system's behavior is observed under successive irradiance levels: 100 W/m², 500 W/m², and 1000 W/m².

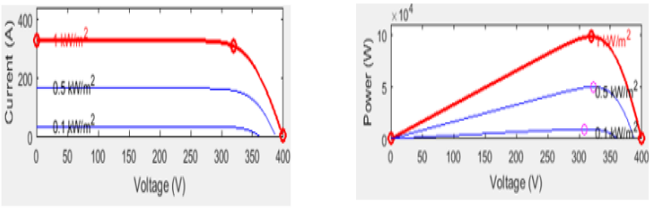

Figure 2: Output Current and Power of the PV Cell as a Function of Voltage

The photovoltaic cell's voltage-dependent power and current features are shown in Figure 2 for various irradiance levels. The cell's output current is shown in another figure. These curves enable us to examine the cell's operating mechanism in relation to the applied voltage.

C. Photovoltaic Panel Module

Photovoltaic cells are the basic building blocks of a solar generator. Since the power output of a single cell is very low, it is necessary to group them together. A set of cells forms a module, multiple modules make up a solar panel, and the assembly of several panels constitutes a photovoltaic array.

TABLE 1: Types of PV Cell Connections and Their Electrical Characteristics

Connection Type	Main Purpose	Electrical Condition	Main Formula
Series	Increase voltage	Same current through each cell	$V_{sco} = N_s \times V_{co}$ (3)
Parallel	Increase current	Same voltage across each cell	$Iscc = Np * Icc$ (4)
Series-Parallel (Mixed)	Increase voltage and current	Series cells: same I_{cc} Parallel cells: same V_{co}	$\begin{cases} Vpv = \sum_{i=1}^{p} Vi \\ Ipv = \sum_{i=0}^{s} Ii \\ Ppv = Np \times Ns \times Vi \times Ii \end{cases}$ (5)

D. Boost Converter

The Boost converter is a step-up DC-DC converter that raises a low input DC voltage to a higher output voltage. It mainly consists of a switch (S), an inductor (L), a diode (D) that protects the photovoltaic array by preventing reverse current flow, and a capacitor (C_2) used to smooth the output voltage, [8].

E. Maximum Power Point Tracking (MPPT) Method

The photovoltaic (PV) system behaves as an intermittent source, since its power output depends on variations in irradiance and temperature. The PV generator can function in a variety of modes: short circuit, open circuit, or maximum power point (MPP), [9].

TABLE 2: Boost Converter Operating Principle

Switch State	Time Interval	Circuit Behavior	Main Formula
Closed (IGBT ON)	$t \in [0, T]$	Diode is reverse-biased; the inductor stores energy	$I_L(t) = \frac{Vpv}{L} t + Im$ (6)
Open (IGBT OFF)	t∈ $[T_S, T]$	Inductor releases energy to the load; output voltage is boosted	$\frac{V_{dc}}{V_{PV}} = \frac{Ipv}{Is} = \frac{1}{1-\alpha}$ (7)

a. P&O Method Flowchart

The voltage V and current III are measured to calculate the instantaneous output power $P(k)$ of the PV string. This value is then compared with the previously measured power $P(k-1)$.

- If $P(k) > P(k-1)$, it means that the power has increased. The voltage perturbation continues in the same direction as in the previous cycle.
- If $P(k) < P(k-1)$, it indicates a decrease in power. The perturbation direction is then reversed compared to the previous cycle.

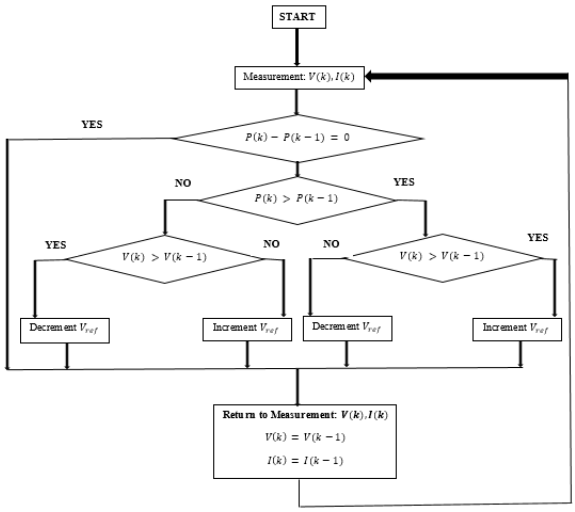

Figure 3: Flowchart of the P&O Algorithm

b. MPPT Control via Pulse Width Modulation (PWM)

The MPPT control is performed using Pulse Width Modulation (PWM) [16]. This technique is based on the comparison between a reference signal (generated by the P&O algorithm, corresponding to the setpoint voltage V) and a carrier signal, usually a high-frequency triangular waveform. The output voltage of the PV generator is then related to the duty cycle α\alphaα by the following formula:

$$V_{PV} = (1 - \alpha) V_{dc} \quad (8)$$

c. DC Bus

The DC bus is represented by a capacitor placed between the photovoltaic (PV) generator and the voltage inverter. The voltage across this capacitor depends both on the duty cycle α of the DC/DC converter and on its output current, which also corresponds to the input current of the inverter.

In the event of a grid-side short circuit, the grid voltage drops, leading to a decrease in the injected power PPP. However, the power produced by the PV panels Ppv remains constant for a certain period. This imbalance causes energy to

Andry Thierry RANDRIANARINOSY, Jean Marc Fabien Sitraka RANDRIANIRINA, Falinirina ANDRIANJATOVO, and Zely Arivelo RANDRIAMANATANY, "Photovoltaic Power Injected into Low Voltage Grid Using P/Q Regulation Method," *International Research Journal of Advanced Engineering and Science*, Volume 10, Issue 4, pp. 9-15, 2025.

International Research Journal of Advanced Engineering and Science
ISSN (Online): 2455-9024

accumulate in the capacitor C, resulting in a rapid increase in voltage V, which may exceed the permissible thresholds, [9].

$$Ppv = Pc + Pres \quad (9)$$

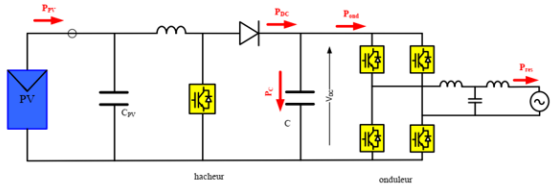

Figure 4 : Power Balance

F. Modeling of the Three-Phase Inverter and LCL Filter

The conversion process is carried out through the switching of semiconductor devices such as IGBTs or MOSFETs. These switches are controlled by rectangular pulse signals generated through the modulation of a reference signal, which represents the desired output voltage waveform of the inverter.

To prevent internal short circuits, the two switches in the same inverter leg must never conduct simultaneously. The operation of the inverter is thus based on eight possible switching states, which include the switches S1 through S6 in a three-phase inverter. By alternating between these eight states, the inverter converts the input DC voltage V_{DC} into an AC output voltage with the desired waveform, [10].

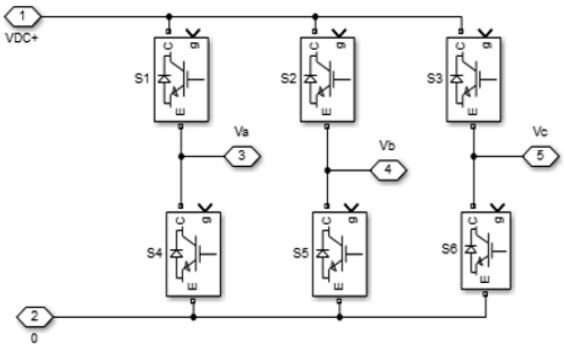

Figure 5 : Three-Phase Inverter

TABLE 3 : Eight Operating States of the Three-Phase Inverter

Etats	Vab	Vbc	Vca	Va	Vb	Vc
$(S1,S2,S3)$ Conduisent et $(S4,S5,S6)$ bloquées	0	0	0	0	0	0
$(S1,S5,S3)$ Conduisent et $(S4,S2,S6)$ bloquées	V_{DC}	-V_{DC}	0	$\frac{V_{DC}}{3}$	$\frac{-V_{DC}}{3}$	$\frac{V_{DC}}{3}$
$(S1,S5,S6)$ Conduisent et $(S4,S2,S3)$ bloquées	V_{DC}	0	-V_{DC}	$\frac{2V_{DC}}{3}$	$\frac{V_{DC}}{3}$	$\frac{-V_{DC}}{3}$
$(S1,S2,S6)$ Conduisent et $(S4,S5,S3)$ bloquées	0	V_{DC}	-V_{DC}	$\frac{V_{DC}}{3}$	$\frac{2V_{DC}}{3}$	$\frac{-2V_{DC}}{3}$
$(S4,S2,S6)$ Conduisent et $(S1,S5,S3)$ bloquées	-V_{DC}	V_{DC}	0	$\frac{-V_{DC}}{3}$	$\frac{V_{DC}}{3}$	$\frac{-V_{DC}}{3}$
$(S4,S2,S3)$ Conduisent et $(S1,S5,S6)$ bloquées	-V_{DC}	0	V_{DC}	$\frac{-2V_{DC}}{3}$	$\frac{-V_{DC}}{3}$	$\frac{V_{DC}}{3}$
$(S4,S5,S3)$ Conduisent et $(S1,S2,S6)$ bloquées	0	$-V_{DC}$	V_{DC}	$\frac{-V_{DC}}{3}$	$\frac{-2V_{DC}}{3}$	$\frac{2V_{DC}}{3}$
$(S4,S5,S6)$ Conduisent et $(S1,S2,S3)$ bloquées	0	0	0	0	0	0

The output voltages of the inverter are square-wave signals with discrete positive and negative amplitude levels. Despite the fact that the waveform looks like a sinusoidal signal, it has a significant total harmonic distortion (THD). Therefore, a filter is required to eliminate the harmonic components.

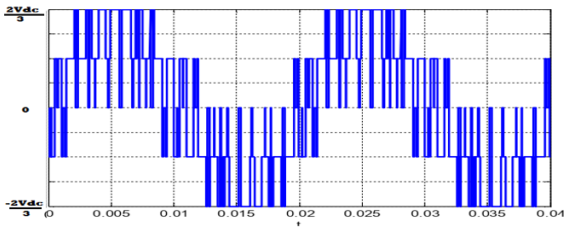

Figure 6 : Phase Voltage at the Inverter Output

A pure LCL filter is generally unstable due to its gain peak and resonance, which can result in a phase margin exceeding –180° a sign of open-loop instability. This resonance creates issues that must be mitigated. A common passive method is to add a damping resistor, either in parallel with the inductor or capacitor, or in series with the capacitor. In this study, the chosen solution is to place a resistor r_c in series with the capacitor C. There are also active methods available to attenuate this resonance.

$$\frac{ig}{Va} = \frac{Cr_cs+1}{CL_1L_2s^3+Cr_c(L_1+L_2)s^2+(L_1+L_2)s} \quad (9)$$

G. The P/Q regulator

The P/Q regulator controls the active and reactive power injected into the grid. Its objective is to maximize active power and to minimize or even eliminate reactive power. It takes into account the power factor of the PV generation, [12].

The regulator begins by setting the active power (P) and reactive power (Q) references, then calculates the reference currents I_{dref} and I_{qref} according to the set points. These reference currents are then compared to the actual currents injected at the point of common coupling, with the reactive power reference set to zero. The resulting difference is used to regulate the inverter voltages V_{dref} and V_{qref}. These voltages are transformed into three-phase reference signals V_{aref}, V_{bref} and V_{cref} through the inverse Park transformation, and then modulated to generate the switching control signals, [13].

In the d-q synchronous frame, the active (P) and reactive (Q) powers are calculated as:

$$\begin{cases} P = \frac{3}{2}(V_d.I_d + V_q.I_q) \\ Q = \frac{3}{2}(V_d.I_d - V_q.I_q) \end{cases} \quad (10)$$

The reference currents are then computed from the set points P_{ref} and P_{ref} using inverse Park transformation and assuming V_d (aligned with the d-axis):

$$\begin{cases} I_q^{ref} = -\frac{2}{3}\frac{Q_{ref}}{V_d} \\ I_d^{ref} = \frac{2}{3}\frac{P_{ref}}{V_d} \end{cases} \quad (11)$$

These references are compared with the measured I_d and I_q the error signals are regulated using PI controllers to generate the inverter voltage references.

III. Simulation of a Grid-Connected PV System Using Matlab/Simulink

The plant consists of a 100 kW photovoltaic system, connected to a Boost converter with MPPT control based on the "Perturb and Observe" algorithm. A three-phase inverter is

Andry Thierry RANDRIANARINOSY, Jean Marc Fabien Sitraka RANDRIANIRINA, Falinirina ANDRIANJATOVO, and Zely Arivelo RANDRIAMANATANY, "Photovoltaic Power Injected into Low Voltage Grid Using P/Q Regulation Method," *International Research Journal of Advanced Engineering and Science*, Volume 10, Issue 4, pp. 9-15, 2025.

International Research Journal of Advanced Engineering and Science
ISSN (Online): 2455-9024

integrated along with its control system, and a grid filter is added to limit harmonics. The system is connected to a 400 V three-phase grid.

In the Malagasy context, solar irradiation varies between 100 and 1000 W/m² and temperature ranges from 10 to 30 °C throughout the day. In Matlab/Simulink, these variations can be modeled over a defined time period using the *Signal Builder* block.

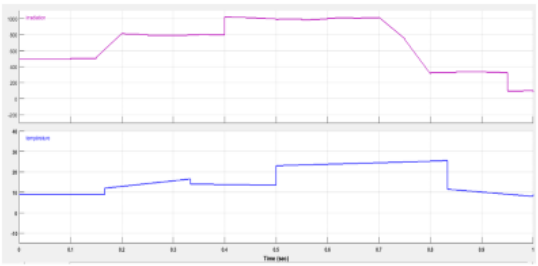

Figure 7 : Irradiance and Temperature Variation Using the Signal Builder Block

The Array PV block in Matlab/Simulink allows the modeling of different types of solar panels. The selected panel is the 1SolTech 1STH-125-P (216.15 W, 36.5 V open-circuit voltage, 7.6 A short-circuit current). The photovoltaic field consists of 39 parallel strings, each with 12 modules in series, resulting in a total power output of 101,089 W.

A DC bus voltage of 600 V is required to supply a three-phase inverter delivering a phase voltage of 400 V. Grid synchronization is ensured by a Phase-Locked Loop (PLL) combined with the Park transformation, which provides the instantaneous grid parameters: phase angle (θ), frequency (ω), and voltage amplitude (V_d).

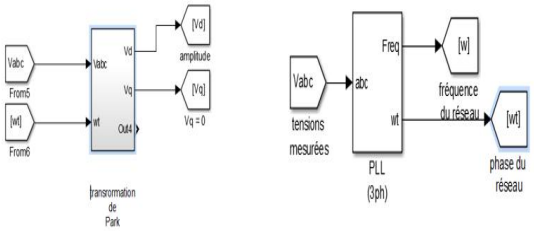

Figure 8 : PLL Block and Park Transformation

The process begins with the calculation of the reference active and reactive power. The reference active power is the sum of the power from the PV module and the power to be injected into the DC bus, while the reactive power reference is set to zero under the P/Q control strategy. The reference currents I_{dref} and I_{qref} are then determined, representing the active and reactive components respectively. These are compared with the measured currents, and the differences are processed by regulators to generate the inverter voltage commands.

The synchronization angle θ\thetaθ, obtained from the PLL and used in the inverse Park transformation, enables the generation of the three-phase reference voltages V_{aref}, V_{bref} and V_{cref}. Finally, the inverter control is performed through modulation, by comparing these reference voltages with a saw tooth waveform.

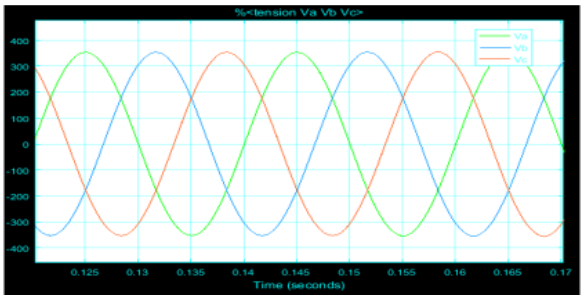

Figure 9 : Waveforms of V_a, V_b and V_c at the Point of Common Coupling

IV. Assumptions and Limitations

The simulation model assumes ideal components without aging effects or manufacturing tolerances. Grid disturbances such as faults, voltage dips, or frequency deviations are not dynamically introduced but considered stable post-fault. The inverter operates at a fixed switching frequency of 10 kHz, and the LCL filter design uses nominal values without adaptive tuning. The damping resistor in the filter is fixed and does not account for thermal variation. These simplifications may affect the applicability of the model in real-world fluctuating grid conditions.

V. Results and Discussions

Table 4 shows that the voltage THD decreased from approximately 17% to 4.29%, and the current THD improved from 20% to 12% after applying the P/Q control strategy. And the power factor increased significantly from 0.25 to a range of 0.4–0.99, while the injected active power reached 99.97% of the PV output and reactive power was reduced to ±250 VAR.

TABLE 4: Comparison of System Performance Before and After P/Q Control

Metric	Before P/Q Control	After P/Q Control
Voltage THD (%)	17	4.29
Current THD (%)	20	12
Power Factor	0.25	$0.4 - 0.99$
Active Power Injected	88% of PV Output	99.97%
Reactive Power (Q)	$\pm 2000\ VAR$	$\pm 250\ VAR$

The total harmonic distortion (THD) of voltage dropped from 17% during transients to 4.29% under steady state, while the current THD remained below 12%. These values align with the IEC 61000-3-2 standard for voltage harmonics in low-voltage grids.

A. Dynamic Behavior of Electrical Quantities in Transient and Steady-State Regimes

The time evolution of voltage, current, and power is visualized using the *"Scope"* block in Matlab/Simulink. A zoom on the oscilloscope enables detailed observation of the waveforms of the three-phase voltages V_a, V_b and V_c at the output of the PV inverter. The simulation runs from $t = 0\,s$ to $t = 0.05\,s$. During this interval, the DC bus charges rapidly, causing initial instability in the production system such as voltage sags, short-circuit currents, and high total harmonic

Andry Thierry RANDRIANARINOSY, Jean Marc Fabien Sitraka RANDRIANIRINA, Falinirina ANDRIANJATOVO, and Zely Arivelo RANDRIAMANATANY, "Photovoltaic Power Injected into Low Voltage Grid Using P/Q Regulation Method," *International Research Journal of Advanced Engineering and Science*, Volume 10, Issue 4, pp. 9-15, 2025.

International Research Journal of Advanced Engineering and Science
ISSN (Online): 2455-9024

distortion. After fault clearance, the system delivers three sinusoidal voltages at the inverter output, synchronized with the grid voltage. The amplitude ranges between 345 V and 370 V, and the frequency lies within the interval [49.5 Hz; 50.5 Hz], with an estimated voltage THD of 5%.

Figure 10 shows that the V_d voltage exhibits transient oscillations before rapidly converging toward zero, confirming the effectiveness of vector control. The V_q voltage reaches a stable value around 350 V from 0.1 s onwards, ensuring proper system operation. The reference voltage V_{dref} remains constant, reflecting accurate regulation. These results validate the stability and performance of the implemented control and conversion system.

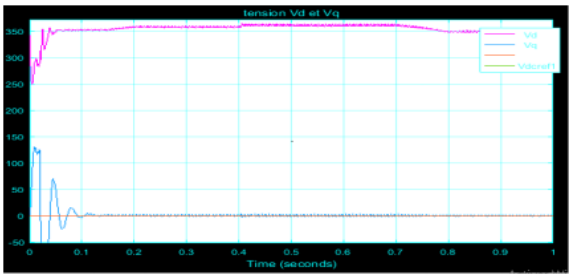

Figure 10: Voltages $\boldsymbol{V_d}$ and $\boldsymbol{V_q}$

Figure 11 presents the evolution of the grid frequency over time. Significant oscillations are observed at startup (up to 0.15 s), indicating transient instability due to abrupt changes in load or production. The frequency then stabilizes around 50 Hz, with slight variations, demonstrating the good performance of the regulation system. This dynamic response highlights the grid's ability to quickly restore balance after a disturbance.

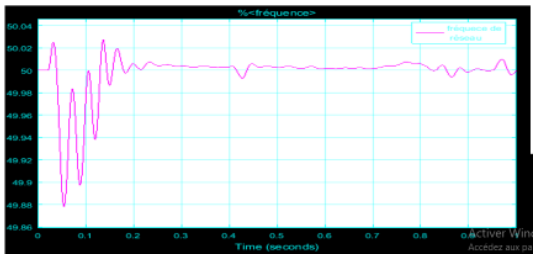

Figure 11: Grid Frequency

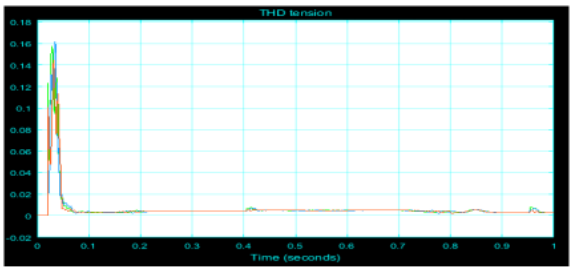

Figure 12 : Voltage THD

Figure 12 illustrates the evolution of the total harmonic distortion (THD) of the voltage over time. An initially high value (approximately 0.17) drops rapidly and stabilizes below 0.02 after 0.1 second. This quick reduction indicates a significant improvement in voltage quality following the transient phase. The studied system effectively reduces harmonics and maintains a nearly pure voltage waveform under steady-state conditions.

B. Output Current of the Inverter

Figure 13 shows the waveforms of the three-phase output currents I_a, I_b and I_c over a short time period (with THD between 10% and 20%). The balance of the three-phase system is confirmed by the three curves' regular sinusoidal shapes, which are phase-shifted by 120°. The constant amplitude and symmetry of the currents indicate a good power quality, with neither imbalance nor distortion. This behavior confirms the system's stability and the effective performance of the control or filtering devices in use.

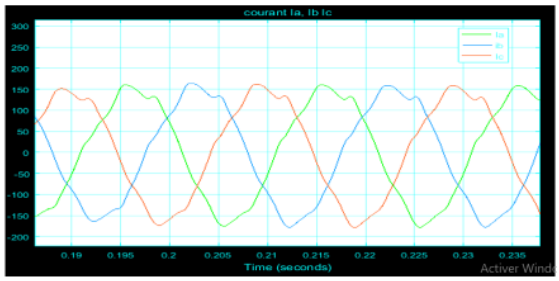

Figure 13: Currents $\boldsymbol{I_a}$, $\boldsymbol{I_b}$ and $\boldsymbol{I_c}$ Injected into the Grid

Figure 14 shows the time evolution of the current components I_d and I_q. Both currents attain a quasi-steady condition after a transient period characterized by high oscillations. The I_q component, associated with torque, remains predominant and well-regulated, while the I_d component, related to flux, remains close to zero. This behavior confirms the effectiveness of the vector control strategy, ensuring clear decoupling between torque and flux.

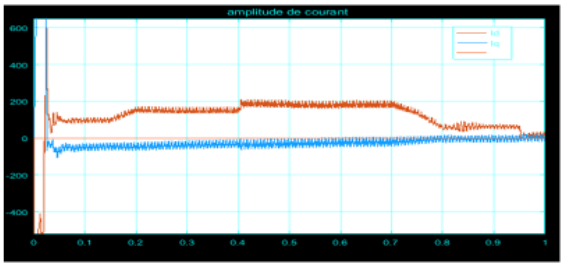

Figure 14: Evolution of Current Components $\boldsymbol{I_d}$ and $\boldsymbol{I_q}$

Figure 15 shows the evolution of active power and the power extracted via the MPPT algorithm over time. The MPPT algorithm efficiently tracks variations in instantaneous power, demonstrating its capability to maximize energy harvesting. Stable plateaus are observed when the maximum power point is accurately reached, despite small oscillations around the optimal value. This performance validates the robustness and effectiveness of the algorithm under varying conditions, confirming the relevance of the proposed model.

Andry Thierry RANDRIANARINOSY, Jean Marc Fabien Sitraka RANDRIANIRINA, Falinirina ANDRIANJATOVO, and Zely Arivelo RANDRIAMANATANY, "Photovoltaic Power Injected into Low Voltage Grid Using P/Q Regulation Method," *International Research Journal of Advanced Engineering and Science*, Volume 10, Issue 4, pp. 9-15, 2025.

International Research Journal of Advanced Engineering and Science
ISSN (Online): 2455-9024

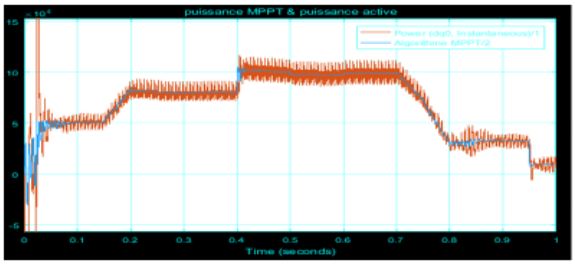

Figure 15 : Power Produced by the PV Field and Active Power Injected into the Grid

Figure 16 presents the evolution of the power factor over time. A gradual decrease is observed, indicating a degradation in energy transfer quality. The significant oscillations at the end of the simulation suggest a possible instability due to perturbations or poor load adaptation. This highlights the need for improved control strategies to stabilize the system and optimize energy performance.

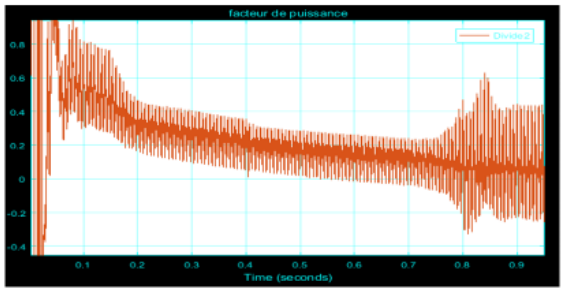

Figure 16 : Power Factor

Figure 17 illustrates the evolution of reactive power over time. Following an initial peak, the reactive power gradually decreases while maintaining slight ripple. This reduction indicates improved system balance and a decrease in energy losses associated with non-active power transfer. The observed behavior confirms the effectiveness of the implemented control in limiting unnecessary energy circulation in the grid.

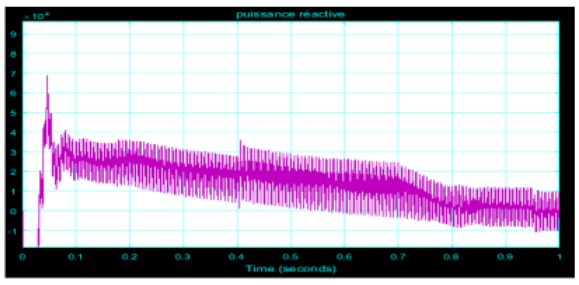

Figure 17 : Reactive Power

The average power factor reaches only 0.4 under low irradiation, which is below the Malagasy GRID-CODE requirement of 0.9 for grid-connected systems. This result highlights a limitation of the current control strategy under reduced solar input. To comply with regulations, future designs should integrate reactive power compensation or implement adaptive control strategies.

TABLE 5: Power Produced by the PV Field under Different Irradiation Levels

Irradiation (W/m^2)	Power Supplied by the 100 kW PV Generator Using the P&O Algorithm (en W).
500	50 000
800	80 000
1000	100 162
300	31 000
100	11 000

Fig.18 illustrates the time evolution of the DC bus voltage Vdc during system start-up. After an initial peak of approximately 800 V, the voltage drops sharply and then stabilizes around 600 V in less than 0.1 second, reflecting the regulator's fast response. Minor oscillations persist, indicating a well-controlled transient regime. Thus, Fig.18 highlights the effectiveness of the voltage control strategy in handling initial disturbances.

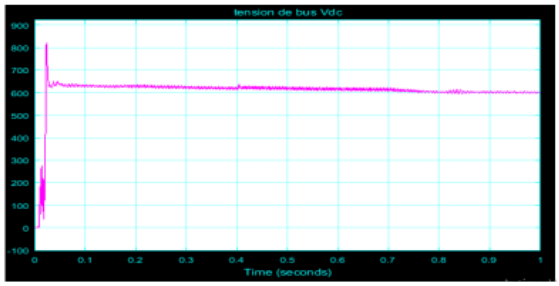

Figure 18 : DC Bus Voltage

The adopted control strategy is local and, based on simulation results, enables the system to generate sinusoidal voltages and currents synchronized with the grid at a frequency close to 50 Hz at the inverter output. This validates the inverter's proper functioning and the PLL loop's ability to synchronize with the grid. The P&O algorithm enables the PV field to reach its maximum power according to irradiation levels, thereby ensuring optimal efficiency. However, due to the absence of energy storage, the generated power is not constant. The system also injects reactive power, explaining the gap between the active power injected and the actual power produced by the modules. Nevertheless, the power factor of 0.4 complies with the grid connection requirements.

Regarding power quality, the voltage at the point of common coupling ranges between 345 V and 370 V, which corresponds to 0.85 to 0.95 pu within the acceptable limits of the Grid Code (0.9 to 1.1 pu) when irradiation is between 400 and 1000 W/m². During periods of low sunlight, this range is temporarily not maintained. Finally, the total harmonic distortion remains below 5%, which is acceptable for the Malagasy electrical grid.

We selected a 600 V DC bus and 400 V phase voltage to meet the Malagasy GRID-CODE for low-voltage integration, which allows voltage variations between 0.9 and 1.1 pu. A PLL is used to ensure synchronization with the grid, following IEEE Std 1547. The 2 Ω damping resistor in the LCL filter helps reduce resonance, in line with standard design practices and local simulation benchmarks.

Andry Thierry RANDRIANARINOSY, Jean Marc Fabien Sitraka RANDRIANIRINA, Falinirina ANDRIANJATOVO, and Zely Arivelo RANDRIAMANATANY, "Photovoltaic Power Injected into Low Voltage Grid Using P/Q Regulation Method," *International Research Journal of Advanced Engineering and Science*, Volume 10, Issue 4, pp. 9-15, 2025.

VI. Conclusion

This study has highlighted the technical challenges related to injecting photovoltaic energy into low-voltage distribution networks, particularly in the context of a country like Madagascar, where access to electricity remains a structural challenge. Based on a P/Q control approach integrated into a fully modeled conversion system, the work has demonstrated the relevance of an adapted control strategy to ensure the stability and quality of energy injected into the grid.

The adopted methodology combines rigorous modeling and numerical simulation to evaluate the system's dynamic behavior under realistic conditions. Beyond the observed performances, this work confirms the necessity of designing robust control strategies that comply with grid connection standards.

The strategy's relevance is further supported by comparable international research applying similar techniques to other developing energy markets. This underlines the potential scalability and adaptability of the proposed model beyond Madagascar.

References

[1] IEA, *Global Energy Review 2025 – Electricity*, International Energy Agency, Paris, 2025 : Global electricity demand increased by 4.3 % in 2024.

[2] Shi X., Wang Y., Li J., "Natural resource scarcity, fossil fuel consumption and environmental degradation: reviewing interlinked crises", *Oxford Open Climate Change*, Vol. 1, Article 020, 2025.

[3] World Bank (Seck A., Koménan K., Andriantahina T.), "Powering Madagascar's future: Unleashing private investment to achieve energy goals", *World Bank Blogs*, 20 février 2025.

[4] Moutevelis D., "Voltage Stability and Control of Electrical Distribution Systems with High Penetration of Power Electronic Converters", *arXiv preprint*, 2025 Apr 25, pp. 1–15.

[5] Smith J., Patel R., "*Advanced P/Q control implementations in rural solar PV grids: field case studies in Brazil, India, and sub-Saharan Africa*", IEEE Access, Vol. 12, pp. 14590–14605, 2024.

[6] Smith J., Chen L., "Photon energy and its relation to wavelength in photovoltaic applications", *Journal of Solar Physics*, Vol. 58, Issue 4, pp. 345–360, 2024.

[7] Rakotondrainy M., Randriamiarana F., "Single-diode modelling and parameter identification of PV cells under varying irradiance: a Matlab/Simulink approach", *E3S Web of Conferences*, 2025, ICEGC'2024, Article 00053, 6 pages.

[8] Hayat A., Sibtain D., Murtaza A.F., Shahzad S., Jajja M.S., Kilic H., "Design and Analysis of Input Capacitor in DC–DC Boost Converter for Photovoltaic-Based Systems", *Sustainability*, Vol. 15 No. 7, Article 6321, 2023

[9] Kumar S., Patel R., Singh A., "Modeling and control of photovoltaic systems under varying environmental conditions: A comprehensive review", *Renewable Energy*, Vol. 215, pp. 56-75, 2025.

[10] Nguyen T.H., Le Q.V., Tran P.M., "Modeling and control of DC bus voltage in photovoltaic systems under grid faults", *IEEE Transactions on Industrial Electronics*, Vol. 72, No. 3, pp. 1785–1794, 2025.

[11] Zhang L., Chen Y., "Control strategies and switching schemes for three-phase inverters in photovoltaic systems", *IEEE Journal of Emerging and Selected Topics in Power Electronics*, Vol. 13, No. 2, pp. 1023–1034, 2025.

[12] Diaz M., Lopez J., "Advanced control strategies for P/Q regulation in grid-connected photovoltaic systems", *Electric Power Systems Research*, Vol. 214, Article 108628, 2025.

[13] López M., García J., "Control of grid-connected photovoltaic inverters using dq-reference frame and maximum power point tracking", *IEEE Transactions on Power Electronics*, Vol. 40, No. 1, pp. 789–799, 2025.

Andry Thierry RANDRIANARINOSY, Jean Marc Fabien Sitraka RANDRIANIRINA, Falinirina ANDRIANJATOVO, and Zely Arivelo RANDRIAMANATANY, "Photovoltaic Power Injected into Low Voltage Grid Using P/Q Regulation Method," *International Research Journal of Advanced Engineering and Science*, Volume 10, Issue 4, pp. 9-15, 2025.